Light-in-flight holography with switched reference beams for cross-correlation in deep volume PIV

S.F. Herrmann[1)], M. Geiger[2)], K.D. Hinsch[1)], J. Peinke[2)]

[1)]Applied Optics, [2)]Hydrodynamics
Physics Department
Carl von Ossietzky University Oldenburg
D-26111 Oldenburg – Germany
Fon: (+49) 441-798-3477, Fax: (+49) 441-798-3576
Email: herrmann@uni-oldenburg.de

ABSTRACT

We present a holographic PIV system which extends the standard PIV analysis scheme of two velocity components (2D2C) to the third dimension and overcomes the disturbing background light in deep volume images reconstructed from particle holograms. In a light-in-flight holography (LiFH) setup the short coherence length of a modified laser source is used to suppress light from out-of-focus regions. The whole flow field is recorded at one instant of time, but only a small shell of the object space is reconstructed from a limited aperture on the hologram. A plane inside the virtual image is then digitized by a CCD imaging system. The position in depth of the reconstructed shell can be adapted when a corresponding aperture on the hologram is chosen. Thus imaging in turbid media (e.g. deep volume flow field seeded with particles) is possible not only for visualization but also for PIV analysis if an appropriate tracer density is achieved. As an illustrating example figure 1 shows a visualization of a vortex structure in a boundary layer of an axisymmetric jet obtained with a basic LiFH setup also used for holographic PIV. For this purpose only the nozzle flow has been seeded.

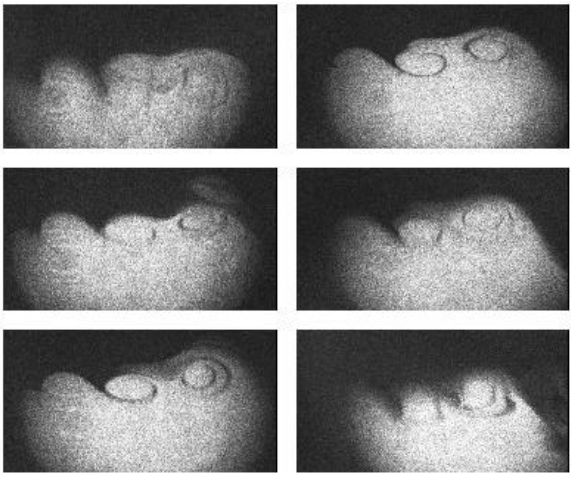

Fig. 1 *Plane-wise sampling of a three-dimensional vortex structure in the boundary layer between an axisymmetric jet and surrounding air. Field of view 44 ´ 70 mm^2, at a distance 30 mm downstream of the nozzle, image planes equally separated over 35 mm depth. The lower field boundary coincides with the nozzle axis.*

For cross-correlation analysis of PIV images two holograms are superimposed on one plate. For this purpose the reference beam direction from a double-pulsed ruby laser is switched between exposures electro-optically by a combination of Pockels cell and a polarizing beam splitter. Cross-correlation algorithms show a much grater tolerance to depth noise and even the LiFH-PIV principle can thus be improved. The novel system is applicable to small scale flows even in turbulent state and offers instantaneous two-dimensional velocity measurements over a deep volume with resolutions well comparable with standard PIV. The performance is demonstrated in studies on the onset of turbulence in a free air flow behind a circular nozzle.

1. INTRODUCTION

Particle image velocimetry has matured into a powerful tool in quantitative flow analysis (Raffel et al.1998). In its basic configuration, the technique yields two velocity components normal to the viewing direction within a thin light sheet placed at proper location and orientation within the flow. PIV setups may be classified according to the number of dimensions involved or more precisely by the number of velocity components (C) and the dimensions (D) of the flow volume inspected (Hinsch and Hinrichs 1996; Stanislas et al. 1999). Thus the original version is termed a 2C2D-technique.

The need for the instantaneous investigation of flow fields in three dimensions has inspired several approaches to extend the well-established concepts of particle velocimetry beyond the plane-wise recording of two-dimensional transversal velocity vectors (Hinsch and Hinrichs 1996). The third component in the sheet volume (3C2D) has been tackled by a variety of approaches. Presently, the most promising method is to combine two traditional PIV recordings at different angles to a stereo image yielding the out-of-plane velocity component. The third dimension can be approached by simply scanning a light sheet through depth in space, the traditional PIV configuration is preserved. However, the recording is not strictly simultaneous and thus the method is restricted to flows that do not change too rapidly in time. Furthermore, a single camera setting must cover the whole depth range which sets limits to the extension of the inspected volume in depth. Yet, impressive results have been obtained in this way (Brücker 1997). Basically, by incorporating stereo in the scanning sheet set-up, a 3C3D-system can be assembled.

For a strictly simultaneous record of particle positions over a region that extends in depth beyond the ordinary depth of focus, holography has proven to be the method of choice. Photographic film of high resolution is a widely used medium for recording holograms. Other holographic recording media like photothermoplastics or photorefractive crystals that can do without laborious chemical and darkroom handling can not cope with the properties of photographic film. An obvious disadvantage of a three-dimensional recording is that the available light can no longer be concentrated effectively to the limited cross section of a thin sheet, but must be expanded to the much larger cross-sectional area of the volume under investigation. Thus available laser light energy sets limits in size to the extent of the measuring volume, even more because holographic recording material is of rather low photographic speed. Even with powerful lasers, however, typical cross-sectional dimensions do not exceed a few centimeter. The third dimension, namely the depth, is limited due to background noise originating from particle images which are out of focus. Depending on the evaluation technique particle positions may not be detected in tracking algorithms (best focus criteria) or correlation functions may have broadened signal peaks which might merge with peaks from uncorrelated noise (auto- and cross-correlation analysis). In spite of these shortcomings, there are several impressive results in holographic particle velocimetry, commonly abbreviated HPIV (Barnhart et al. 1994; Meng and Hussain 1995; Coria et al. 1999).

2. LIGHT-IN-FLIGHT HOLOGRAPHY (LiFH)

Considerable suppression of the out-of-focus noise is achieved when the so-called light-in-flight holography is used in a PIV setup (Hinrichs et al., 1997). LiFH is based on short-coherence light sources or alternatively on ultra-short laser pulses and has been used to visualize wave fronts in optical setups (e.g. Abramson, 1996). The method can be seen as an analogon to optical coherence tomography (OCT) for imaging in turbid media or coherence radar profiling.

Holography relies on the interference of two light waves, termed object- and reference wave, at the position of the recording medium. The resulting intensity modulation is recorded, serves as a diffraction grating during reconstruction and causes light from the reference beam to rebuild the object wave. Obviously scattered light from particles (object wave) and the reference wave can interfere only when their path difference is smaller then the coherence length of the light. As shown in figure 2, reference light incident from the left has to travel a longer path to the right side of the holographic plate than to the left. Object light scattered from particles is recorded only if its pathlength differs no more than the coherence length L from the corresponding reference light. Thus, with proper alignment particles from a shell in the middle of the observed field are recorded at a small region in the middle of the plate, particles from a front shell on the left and from a rear shell on the right. Upon reconstruction through a small aperture only a shell with a depth of roughly one half of the coherence length shows up.

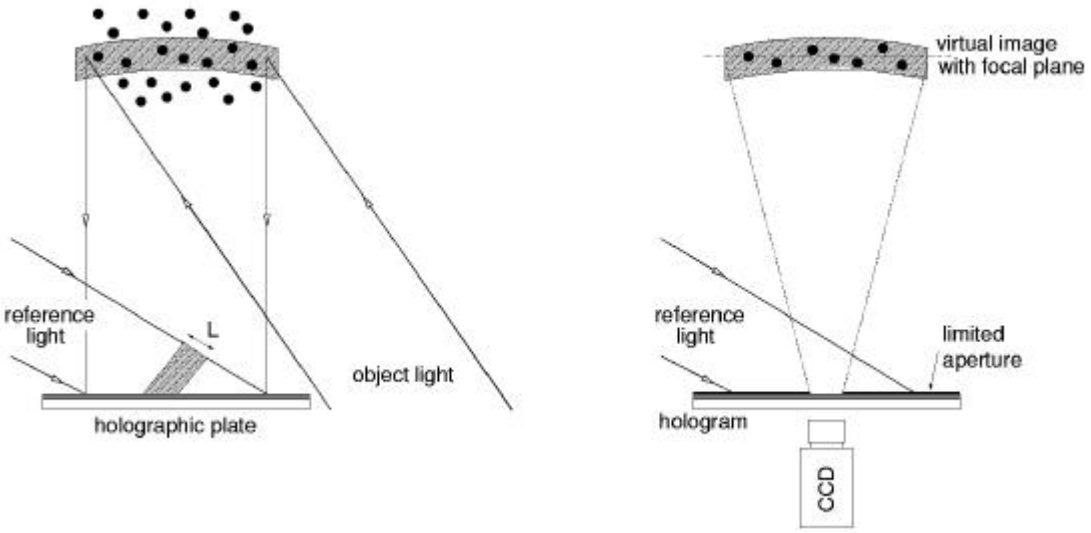

Fig. 2 *Schematic of light-in-flight holography with short coherence length for particle recording (left) and reconstruction of particle images (right).*

For particle recording with the LiFH principle a back-scattering geometry is desired, which additionally limits the illuminated cross-section of the flow due to poor reflection efficiency of tiny tracer particles. We currently use as light source a modified double-pulse ruby laser with energies up to 5 J per pulse. The short coherence length is obtained by removing the etalons leading to approximately 100 longitudinal modes in a 0.7 m resonator. The resulting coherence length can be estimated by a simple experiment. A ruler is placed obliquely at an angle of $g = 45°$ in object space and recorded with a single pulse. Figure 3 shows the resulting image when the ruler is reconstructed through small apertures at three different positions on the hologram. From geometrical relations the coherence length is calculated to be $L \approx d \times \cos g \approx 7$ mm, where d is the width of the reconstructed part on the ruler.

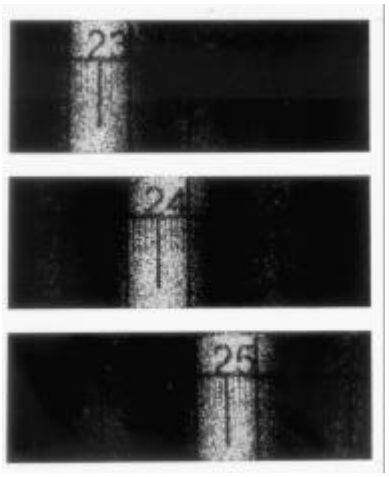

Fig. 3 *Demonstration of the limited reconstructed object depth due to the short coherence length of the ruby laser. A ruler is recorded with an object wave incident at 45° and reconstructed from different apertures on the hologram. The coherence length is approximately 7 mm.*

If light scattered from tiny particles is recorded with the above mentioned principle quasi two-dimensional images can be extracted afterwards. The efficiency in suppressing light from undesired regions is well demonstrated in a visualization of the vortex structure in the boundary layer between a free air jet and the surrounding air (figure 1). The ring-vortex structure has been observed 30 mm downstream behind a circular nozzle with a diameter $D = 50$ mm at an average velocity of $v = 2$ m/s and $Re \approx 7500$. The lower boundary of the field of view (44×70 mm^2) is given by the axis of the jet. Image planes are equally separated over 35 mm in depth. From upper left to lower left the ring-vortex is first oriented more perpendicular to

the viewing direction and cut parallel afterwards. Following, the rear part of the jet is shown on the right side, where the vortex is finally oriented perpendicular again.[1]

The use of light-in-flight holography for quantitative flow velocimetry has been demonstrated in a study of irregular vortex shedding behind a cylinder in a wind tunnel using water-glycerin particles of a few µm in diameter (Hinrichs et al. 1998b). Auto-correlation analysis was used in this study to evaluate the double exposure light-in-flight holograms which basically restricts the dynamic range of the system and requires a minimum particle displacement to ensure correct measurements.

3. CROSS-CORRELATION ANALYSIS IN HPIV

Early PIV used the superposition of both exposures and auto-correlation analysis. Later, the obvious advantages of cross-correlation processing (Kean et al. 1992) led to its general acceptance and have made it standard in digital PIV (DPIV). There is a considerable increase in the rate of valid velocity vectors and their directions are no longer ambiguous. In HPIV cross-correlation has been introduced because of the same reasons. The above mentioned noise problem from out-of-focus particles is greatly relaxed as numerical and experimental results show a much greater tolerance to depth-noise in cross-correlation analysis (Hinrichs et al. 1998a). Validation rates above 90 – 95 % are commonly considered sufficient for a proper vector post-processing (e.g. outlier removal, hole filling, median filtering and vorticity estimation). Figure 4 illustrates that cross-correlation analysis is advantageous in analyzing images from a deep flow field, where light sheets or illuminated volumes reach 5 mm and more in depth.

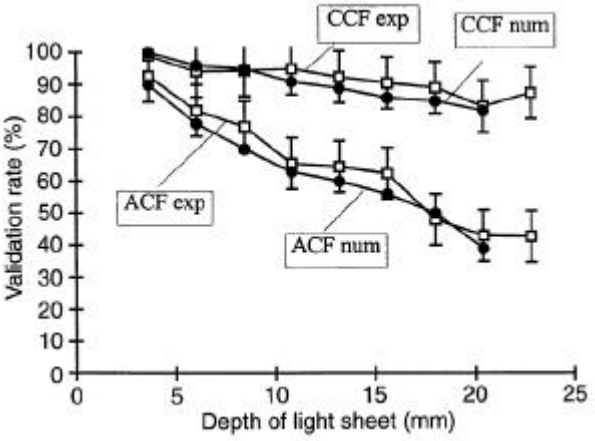

Fig. 4 *Validation rates vs. depth of flow field. Comparison of numerical simulations and experimental model for evaluation by auto- and cross-correlation, from (Hinrichs et al. 1998a).*

The considerable gain between auto- and cross-correlation, even for a depth of some 10 mm, points the way to improve even LiFH-PIV. To provide separable images for each laser pulse two basic schemes have been used in holography. The first method is commonly termed spatial multiplexing. With reference beams smaller in cross-section than the dimensions of the holographic plate two different positions on one plate can be used to store two discrete holograms. In contrast the use of reference beams of different angles (angular multiplexing) offers the superposition of two or more holograms in the same region of the plate.
The angle of incidence for each hologram has to be chosen carefully to avoid cross-talk of images. In the observation of the virtual image only one position of the CCD camera is needed to digitize both images for t and $t + \Delta t$ from the same aperture thus bewaring of laborious adjustment.

[1] An animated visualization with a total of 21 frames covering a depth of 46 mm can be found at http://hbar.physik.uni-oldenburg.de/piv

4. SETUP WITH ELECTRO-OPTICALLY SWITCHED REFERENCE BEAM

In our setup the reference beam direction from a double-pulsed ruby laser is switched between exposures. Pulse separation is 10 – 500 µs, typically, so rapid switching is required suggesting acousto-optic or electro-optic configurations. We have found the later solution of advantage. Adjustment and control of the switching devices proves much easier for a Pockels cell due to larger aperture sizes, higher damaging threshold and TTL based electronics to trigger a high voltage pulse for the switching. The advantage in using an acousto-optic device for beam steering could be seen in the possibility to handle more then two reference beam directions, a feature not required presently.

As shown in figure 5, the initially vertical polarization of the laser light is rotated for the second pulse by the Pockels cell yielding two different reference beams behind a polarizing beam splitter.

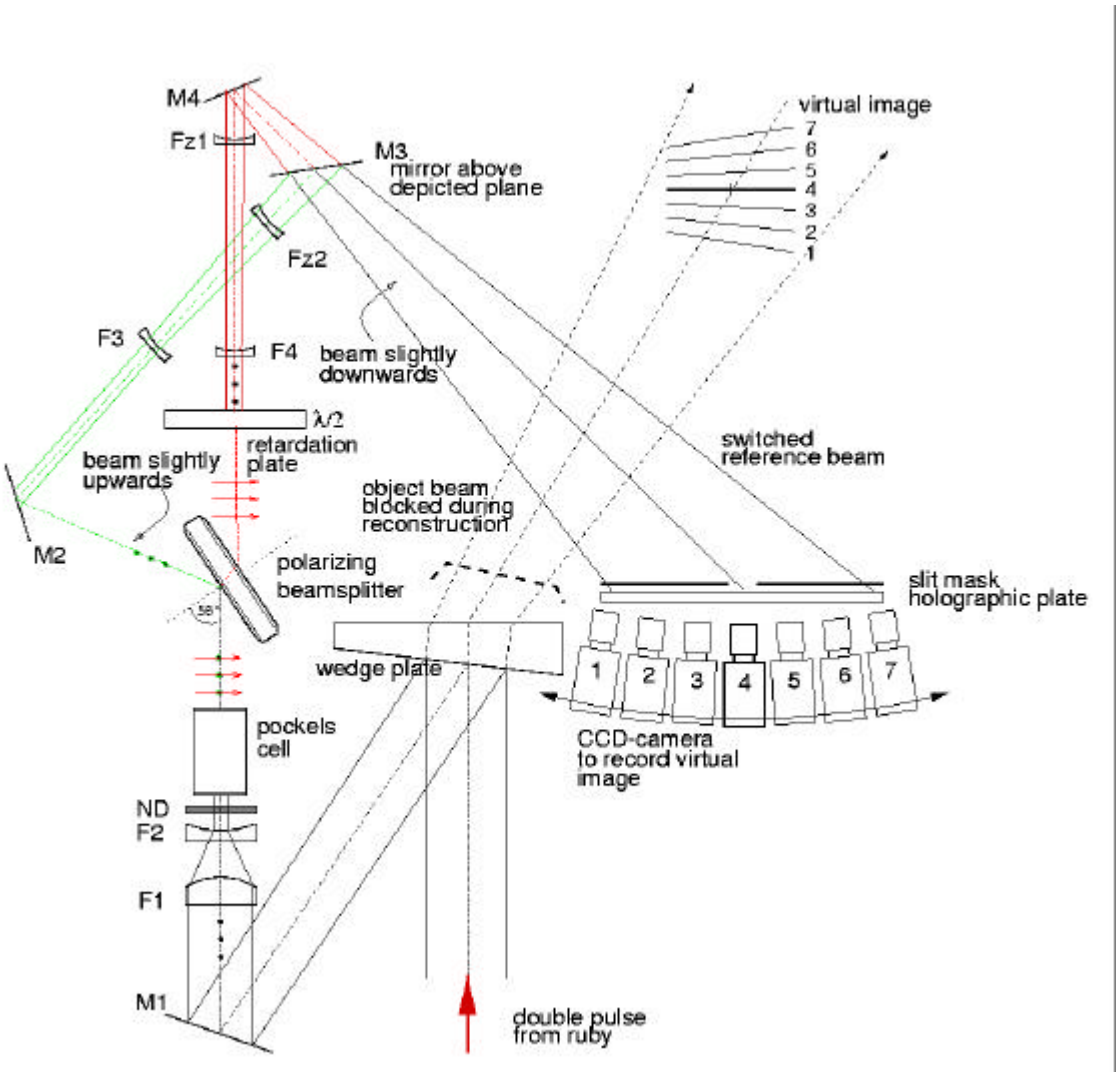

Fig. 5 *Light-in-flight setup for recording with polarization-switched reference beams offering different angles of incidence. The reflected reference beam expanded by lens F3 projects out of the paper plane to fall onto the holographic plate from above. Sheet-wise reconstruction is done with the same setup by blocking one reference beam direction and the object beam. In-focus planes in depth correspond to the horizontal position of the CCD camera.*

For holography the rotated polarization has to be restored to its original state with a retardation plate to provide for the property of interference with the object beam. The horizontal component of the angle of incidence has to be kept the same for both directions of the reference beam. This ensures that from one aperture on the holographic plate the same shell in object space is reconstructed if path-lengths are made equal. Thus, the reference beam reflected from the beam splitter is

directed out of the paper plane to fall onto the plate from slightly above. This requirement restricts the freedom in designing LiFH setups.

Reconstruction is done in the same setup with the pulsed ruby laser to avoid image distortion from the unmatched wavelength of another laser. Therefore the object beam and one of the reference beam directions are blocked by a dumper. The position of the reconstructed shell and the imaged object plane is determined by geometrical relations from the position of the reconstructing aperture on the holographic plate. This in turn is linked to the viewing direction of the CCD camera as depicted in figure 5, resulting in slightly tilted sheets with increasing depth.

5. MEASUREMENTS OF A FREE JET IN AIR – TRANSITION TOWARDS TURBULENCE

To demonstrate the ability of the LiFH-PIV system a turbulent free flow from a circular nozzle (for details of the flow configuration see below) was measured requiring a high dynamical range. The cross-correlation evaluation was done with a basic algorithm in 64×64 px^2 interrogation areas with 75% overlap, yielding 3600 vectors from a 1008×1016 px^2 image (figure 6). Vector validation according to the recommendation from Keane & Adrian (1992) has been used to discard vector data with SNR < 1.2 Validation rates comparable to those predicted in the simulation were observed. For the best hologram an average of 97% from 18 different shells, equally spaced over the entire object space, even surpasses the prediction of 95% if a depth of the reconstructed field of 10 mm is assumed (refer to figure 4, the coherence "depth" is approximatly 10 mm).

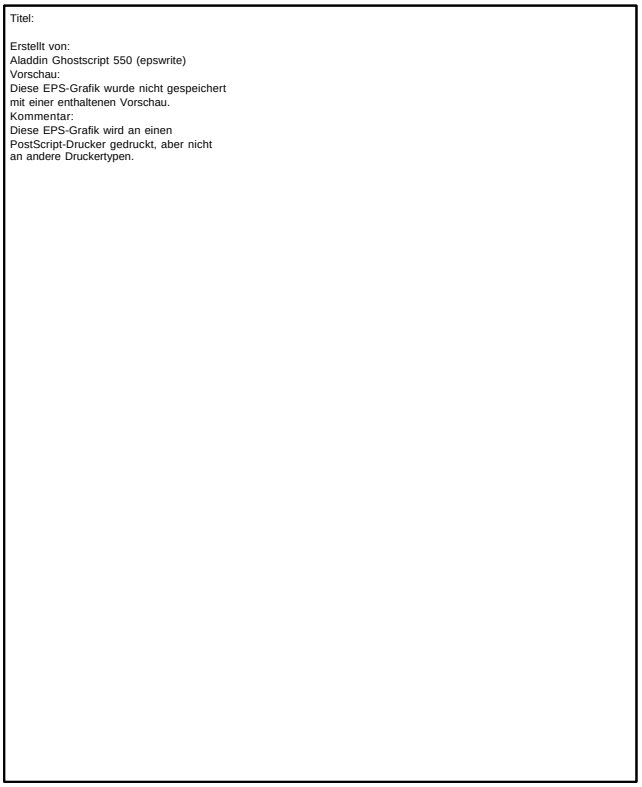

Fig. 6 *Free air flow from a circular nozzle: one selected sheet near the flow axis with 3600 vectors, field of view 35 ´ 35 mm^2, no mean velocity subtraction, no vector post-processing.*

A corresponding auto-correlation analysis was simulated on one synthetic frame produced by simply adding two corresponding frames from the experiment. The minimum displacement required for proper correlation-signals is not achieved in regions of the ambient fluid leading to validation rates much below the model value. Thus comparison of real flow experimental data with the model prediction has to be done in further experiments with proper flow configurations for auto-correlation PIV algorithms (e.g. wind tunnel experiment).

In transition research the development of large-scale structures is of basic interest. The temporal evolution is most often examined with hot-wire anemometry (HWA) which sets limits to spatial resolution and does not permit the instantaneous recording of the spatial velocity distribution. We used LiFH-PIV to localize these structures and calculate their corresponding fluid dynamical quantities (e.g. shear, vorticity and normal strain). Figure 7 shows a visualization of the investigated free jet in air from a circular nozzle with an outlet diameter of D = 8 mm. The transition from mostly laminar flow into turbulence is showing a wavelike structure develop from the helical mode of the free jet. Areas covered by our measurements are indicated by arrows. The laminar flow (a) was measured at a distance of 5D at Re = 340 and the region towards higher turbulence (b) at a distance of 14D at Re = 1200. Both flow configurations have been investigated in volumes of about $35 \times 35 \times 25$ mm^2 each sampled by 19 equally spaced sheets.

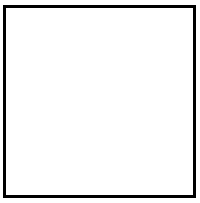

Fig. 7 *A visualization of the examined free jet. The jet looks similar at Re=340 and Re=1200 while the length of the different regions is varying of course. Arrows indicate the corresponding regions where holograms have been taken, (a) the mostly laminar region and (b) transition towards turbulence.*

As an example we show in figures 8 & 9 the distribution of vorticity (a) and shear (b) for both cases in a plane near the flow axis. In the laminar case (figure 8) the spatial distribution of both quantities is similar, as the subtraction (c) of absolute values shows a uniform distribution. The transition region (figure 9) can be identified by spatial decorrelation of shear and vorticity (i.e. the subtraction shows spots with higher magnitudes). Detected local events are marked by arrows, regions with dominating vorticity (I) or shear (II) are observed as well as regions of equal magnitudes of both quantities (III).

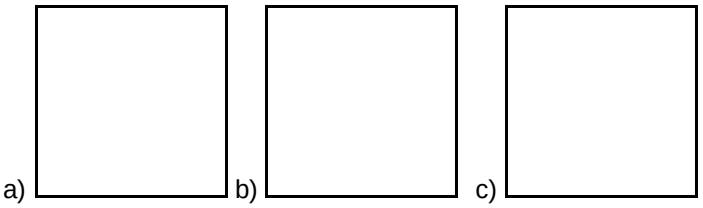

Fig. 8 *Laminar case at Re=340, colors representing in-plane (a) vorticity and (b) shear of the velocitiy field. (c) is a subtraction of absolute values of vorticity and shear. Small arrows indicate the local velocity vectors.*

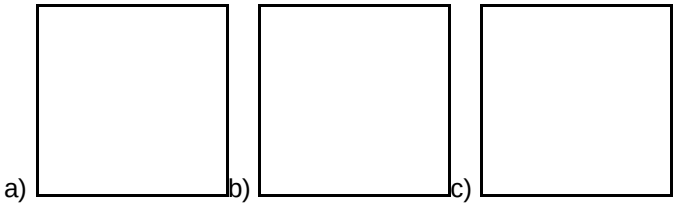

Fig. 9 *Turbulent case at Re=1200, colors representing in-plane (a) vorticity and (b) shear of the velocitiy field. (c) is a subtraction of absolute values of vorticity and shear. Big arrows are indicating regions of (I and II) rotation-shear separation and (III) equal magnitude of rotation and shear.*

Structures of the boundary layer of a laminar jet can be observed from the calculation of the normal strain component. For non-compressible flow the condition $\nabla U = 0$ holds. Thus we are able to calculate the strain component $\partial u_z/\partial z$ from the knowledge of $\partial u_x/\partial x$ and $\partial u_y/\partial y$. In figure 10 this z-strain component is shown for two-dimensional cuts through the evaluated volume of the laminar region in the jet. A finite value of $\partial u_z/\partial z$ indicates local hyperbolic sink- or source-like flow pattern. Most remarkably we find such flow patterns only in the plane tangential to the boundary of the round jet and

not in the center plane. Rotating vortex rings around the jet could be at the origin of the normal strain patterns shown in figure 10 (Rupp, 2000).

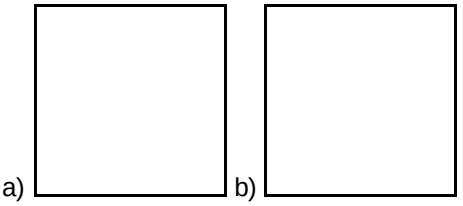

Fig. 10 *Normal strain component for (a) the tangential plane and (b) a center plane of laminar jet*

In addition the probability density functions (pdf) of velocity increments $v_r = u(x-r) - u(x)$ on different scales r are calculated for the central plane of the turbulent field. The well known effect of turbulence, that the distributions become more intermittent towards smaller scales r can be seen. This means that large velocity increments appear more frequently and the peak is sharpening as the scale r decreases (figure 11) (Lück, 1999).

First insight in the depth structure of turbulence is obtained from the LiFH-PIV measurement presented here. Fully independent sheets, however, must at least be separated by a 6 mm distance. This is caused by a rather large focal depth of the used imaging system due to the restrictions from LiFH, requiring small apertures on the hologram. As a result we observe an averaging effect on local velocities, but still a development in depth can be analyzed with appropriate visualization tools. For this purpose the raw data from cross-correlation analysis was reorganized in a three-dimensional space considering the orientation of sheets relative to each other. Various techniques, like iso-surfaces of equal velocities or corresponding dynamical quantities, can then be used to visualize the three-dimensionality. A rather simple but powerful starting point is a moving sheet through the volume retaining the well-established view of particle image velocimetry (figure 12). Assembled in a short animation this technique allows a quick inspection of deep volume flows.

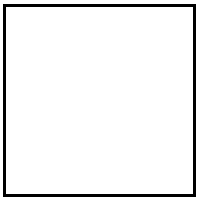

Fig. 11 *Normalized probability density functions (pdf) of velocity increments on different scales, shifted along y axis for clearness of presentation.*

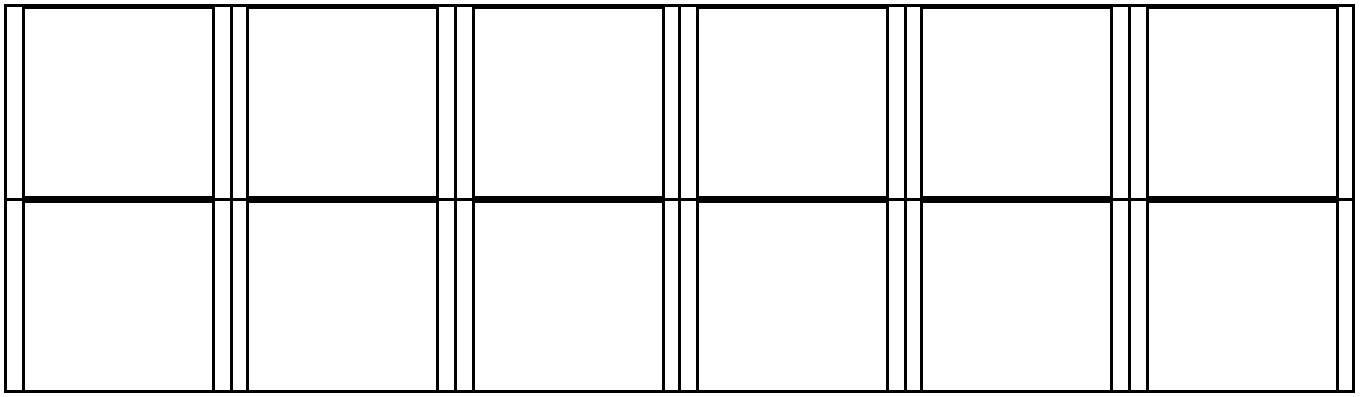

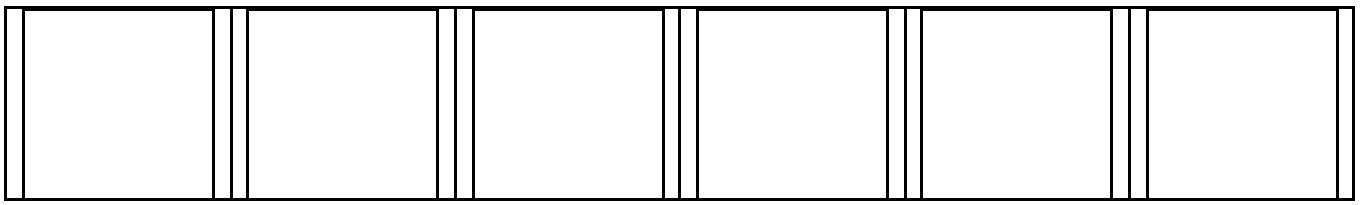

Fig. 12 *Extracted scenes from an animated visualization to observe changes in the depth structure.*

6. CONCLUSIONS AND OUTLOOK

Light-in-flight holography of particle fields in flows has turned out to be a versatile instrument in the handling of three-dimensional flow fields that extend over a large depth of field and require instantaneous recording for a velocity map. While the experimental configurations can still be improved in various ways, already now results are superior in quality to data obtained by other three-dimensional methods. There are some possible modifications that promise immediate progress in the technique and there are also additional options for further development. Some of these are:

1. The assembly of the evaluated sheets into a velocity map of the complete measuring space requires delicate alignment when virtual images are observed. Translation of the CCD-camera behind the hologram to change the position of the reconstructing aperture shifts the observation field accordingly which must be corrected by an appropriate tilt of the camera. Alternatively, it is much easier to assemble sub-volumes in real-image space which, however, requires a conjugate complex reconstructing wave of high fidelity.

2. Obviously, the size of the holographic recording medium limits the field depth. Subdivision of the holographic plate in combination with two or more temporally delayed reference waves provides a way to overcome such restrictions. In this way, area on the plate that has not been used till then is made optimum use of.

3. For third-component analysis stereo evaluation of holographically reconstructed particle sheets is desirable. In LiFH, however, changing the viewing position on the holographic plate usually means observing a different depth-region in space. For a horizontal plane of incidence of the reference wave, for example, matched images for stereo evaluation can only be obtained from vertically separated image pairs. A thorough analysis of the geometric situation in LiFH is required to design for optimum use of the space available on the photographic plates traditionally used.

4. Versatility of the holographic method can be increased when relay imaging is made possible. This becomes necessary, for example, when the situation does not allow to approach the object flow close enough. Since light-in-flight holography relies on the distribution of object light over a large area on the plate, image plane holography becomes impossible and the conditions must be analyzed in detail.

5. The suitability of other light sources in LiFH for flow diagnostics must be studied. Our ruby laser pulses of some mm in coherence length proved just right for the present development. Yet, the ruby laser is difficult to handle in practice because its low repetition rate makes optical alignment a time consuming task. Other more available pulsed sources like Nd:YAG lasers will be investigated as to their suitability.

ACKNOWLEDGMENTS

The studies have been supported by a grant from Deutsche Forschungsgemeinschaft, DFG Hi243/18-3 and by EU-funds BR.PR-CT95-0118 (EUROPIV). The authors would like to thank Dr. N. Andres, University of Zaragoza – Spain, for their help during the measurements. S.F. Herrmann would like to acknowledge the financial support of the Wolfgang-Schulenberg-Programm from Universitätsgesellschaft Oldenburg, which enables a contribution to this symposium.

REFERENCES

Abramson, N. (1996). "Light-in-Flight or the Holodiagram: The Columbi egg of Optics". Bellingham, Wash: SPIE Optical Engineering Press

Barnhart, D.H., Adrian, R.J. and Papen, G.C. (1994). "Phase conjugate holographic system for high resolution particle image velocimetry", Appl. Opt. 33. pp.7159-7170

Brücker, Ch. (1997). "3D scanning PIV applied to an air flow in a motored engine using digital high-speed video", Meas. Sci. Technol. 8, pp.1480-1492

Hinrichs, H., Hinsch, K.D., Kickstein, J. and Böhmer, M. (1997). "Light-in-flight holography for visualization and velocimetry in three-dimensional flows". Opt. Lett. 22, pp.828-830

Hinrichs, H., Hinsch, K.D., Kickstein, J. and Böhmer, M. (1998a). "Deep field noise in holographic particle image velocimetry (HPIV): numerical and experimental particle image field modeling". Exp. in Fluids 24, pp.333-339

Hinrichs, H., Hinsch, K.D., Netter, R. and Surmann, C. (1998b). "Light-in-flight particle holography for velocimetry in a wind tunnel", pp.19.1-19.5. In: Carlomagno, G.M. and Grant, I. (Eds) Proc. 8th Intl. Symp Flow Visualization

Hinsch, K.D. and Hinrichs, H. (1996). "Three-dimensional particle velocimetry", pp.129-152. In: Dracos, T. (Ed), "Three-Dimensional Velocity and Vorticity Measuring and Image Analysis Techniques", Amsterdam. Kluver Academic Publishers

Keane, R.D. and Adrian, R.J. (1992). "Theory of cross-correlation analysis of PIV images", Appl. Sci. Res. 49, pp.191-215

Lozano, A., Kostas, J. And Soria J. (1999), "Use of holography in particle image velocimetry measurements of a swirling flow", Exp. in Fluids 27, pp.251-261

Lück, St., Peinke, J. and Friedrich, R. (1999), "Uniform Statistical Description of the Transition to Turbulence between Near and Far Field Turbulence in a Wake Flow", Phy.Rev.Letters, 83, No. 26, pp.5495-5498

Meng, H. and Hussain, F. (1995). "In-line recording and off-axis viewing technique for holographic particle velocimetry", Appl. Opt. 34, pp.1827-1840

Raffel, M., Willert, C.E. and Kompenhans, J. (1998). "Particle Image Velocimetry: a Practical Guide", Berlin: Springer-Verlag

Rupp, P., Gaksch, H., Lück St. and Peinke J. (1999). "On the helical mode in the transition region of a round free jet", submitted to Exp. in Fluids

Stanislas, M., Kompenhans, J. and Westerweel, J. (Eds) (1999). "Particle Image Velocimetry: Progress Toward Industrial Application", Amsterdam: Kluwer Academic Publishers